

<https://doi.org/10.1002/pip.2727>

This is the peer reviewed version of the following article: Peng, J., Curcija, D. C., Lu, L., Selkowitz, S. E., Yang, H., & Mitchell, R. (2016). Developing a method and simulation model for evaluating the overall energy performance of a ventilated semi-transparent photovoltaic double-skin facade. *Progress in Photovoltaics: Research and Applications*, 24(6), 781-799, which has been published in final form at <https://doi.org/10.1002/pip.2727>.

Developing a method and simulation model for evaluating the overall energy performance of a ventilated semi-transparent photovoltaic double-skin facade

*Jinqing Peng^{a, b}, Dragan C. Curcija^c, Lin Lu^{b, *}, Stephen E. Selkowitz^c, Hongxing Yang^b
Robin Mitchell^c*

^a College of Civil Engineering, Hunan University, Changsha 410082, Hunan, China

^b Renewable Energy Research Group (RERG), Department of Building Services Engineering, The Hong Kong Polytechnic University, Hong Kong, China

^c Building Technology and Urban Systems Division, Lawrence Berkeley National Laboratory, 1 Cyclotron Road, Berkeley, CA 94720, USA

*Corresponding author. Tel.: +852 3400 3596; Fax: +852 2765 7198; Email address: bellu@polyu.edu.hk (L. Lu), Jallenpeng@gmail.com (J. Peng).

Abstract

A comprehensive simulation model has been developed in this paper to simulate the overall energy performance of an amorphous silicon (a-Si) based photovoltaic double-skin facade (PV-DSF). The methodology and the model simulation procedure are presented in detail. To simulate the overall energy performance, the airflow network model, daylighting model and the Sandia Array Performance Model (SAPM) in the EnergyPlus software were adopted to simultaneously simulate the thermal, daylighting and the dynamic power output performances of the PV-DSF. The interaction effects between thermal, daylighting and the power output performances of the PV-DSF were reasonably well modelled by coupling the energy generation, heat transfer and optical models. Simulation results were compared to measured data from an outdoor test facility in Hong Kong in which the PV-DSF performance was measured. The model validation work showed that most of the simulated results agreed very well with the measured data except for a modest overestimation of heat

gains in the afternoons. In particular, the root-mean-square-error (RMSE) between the simulated monthly AC energy output and the measured quantity was only 2.47%. The validation results indicate that the simulation model developed in this study can accurately simulate the overall energy performance of the semi-transparent PV-DSF. This model can, therefore, be an effective tool for carrying out optimum design and sensitivity analyses for PV-DSFs in different climate zones. The methodology developed in this paper also provides a useful reference and starting point for the modelling of other kinds of semi-transparent thin-film PV (STPV) windows or facades.

Keywords: Thin-film PV, building integrated photovoltaics (BIPV), semi-transparent photovoltaic windows, overall energy performance simulation, EnergyPlus, double-skin facade

1. Introduction

Buildings consume about 60% of the total electricity used in Hong Kong and this proportion has been increasing in recent years. Among the various types of building energy use, space air-conditioning has accounted for more than 50% [1]. The high energy consumption of air-conditioning can be partially attributed to the extensive use of the glass curtain wall in modern buildings for reasons of aesthetics even though its poor thermal insulation and solar control performance increases the heating/cooling loads significantly. The need to develop energy efficient curtain walls or facades is urgent. While still satisfying aesthetic needs for view and daylight, such energy efficient facades should passively reduce building energy use as much as possible and it would be even better if they can also actively generate electricity by themselves. These expectations of building facades provide a good opportunity for optimized building integrated photovoltaic (BIPV)

facades or windows. BIPV facades/windows refer to the use of glass-substrate semi-transparent PV (STPV) modules to substitute for conventional glazing to constitute the building facades. STPV facades/windows can provide good overall energy performance because they can not only generate electricity via their solar cells but also reduce the solar heat gain considerably [2-5]. Due to these advantages, the energy performance of STPV windows/facades has been extensively investigated, including the heat transfer mechanism [6-7], surface temperature and solar heat gain coefficients [8-9], thermal comfort [10-11], annual thermal and electrical performance [12-15] and lifetime performance [16]. Compared with crystalline silicon (C-Si) based STPV facades/windows, thin-film STPV facades/windows have a better architectural acceptable appearance due to their uniform appearance from both outside and inside, which are almost the same as dark window glazing. In addition, the thin-film STPV facades would not cast shadow in indoor room. Previous studies also showed that thin-film STPV windows/facades would be better than crystalline silicon based STPV windows/facades for office buildings because of their uniform and aesthetic appearance [3, 17]. In particular, with the development of thin-film PV technologies in recent years, greater efficient semi-transparent PV modules with customized sizes, patterns and colors are emerging, providing more choices for architects to take into account in respect of both building energy efficiency and aesthetics when choosing building glazing facades. Hanergy, as one of the biggest global thin-film PV manufacturers, has produced a series of a-Si semi-transparent PV modules with different colors (via changing the color of the encapsulating material), different sizes (cutting the standard 1.3×1.1 m PV module into small size or splicing a few modules into a big one), different transmittances (theoretically any transmittance can be achieved) and different

structures (laminated structure, sandwich structure with a 9 mm gap filled with air or argon, and so on) [18-19]. Advanced Solar Power (ASP), a company specializing in CdTe thin-film PV modules in China, has commercialized some kinds of semi-transparent CdTe modules with high efficiency and high transmittance recently [20]. PV modules with different colors, different sizes and structures can also be customized according to the clients' requirements.

The overall energy performance of an amorphous silicon (a-Si) thin-film STPV window installed on an office building in Hong Kong was evaluated [17]. A 2D heat transfer model was developed to simulate the thermal performance, a simple power output equation was used to calculate the electricity output of the PV module assuming the energy conversion efficiency was constant, and the daylighting performance was simulated by EnergyPlus. With these models and software, the effect of solar cell transmittance on the overall energy performance was studied. It was found that a solar cell visible transmittance in the range of 0.45–0.55 achieves the best energy saving performance [17]. However, it is worth noting that the optimum transmittance is dependent on the PV module's efficiency, the higher the module efficiency, the lower the optimum transmittance. When the PV module's efficiency is very low, the overall energy saving performance of the PV module is mainly determined by the daylighting performance because the PV generated power is very limited. However, with the efficiency improvement of a-Si PV modules in recent years, the PV generated power increases significantly, thus the optimum transmittance for achieving the best energy saving should be declining. Li et al. [21] conducted case studies to investigate the energy performance of a semi-transparent a-Si PV facade based on a generic reference office building in Hong Kong. In this study, the indoor daylighting

illuminance was calculated using the visible transmittance of the PV module, and the solar heat gain was estimated using a shading coefficient. However, the method of calculating the annual electricity generation of the PV system was not reported. The energy saving potential of STPV facades with different window-to-wall ratios and different transmittances was simulated by Olivieri et al. [22]. In this study, the overall energy performances, including thermal, power and daylighting performances, were simulated separately using different software tools. For instance, the thermal analysis was conducted by EnergyPlus, the electricity generation was estimated by PVsyst and the daylighting performance was evaluated using the Optics, WINDOW and COMFEN programs. Didone and Wagner [23] evaluated the energy saving potential of STPV windows in Brazilian office buildings via simulation. The energy consumption of the building was simulated by combining EnergyPlus and Daysim/Radiance programs. The power generation of PV windows was calculated by a spreadsheet program.

The integral energy performances of STPV windows with different transmittances were measured under real operational conditions in Spain [24]. The thermal, luminous and electrical performances of STPV windows with visible transmittances ranging from 10% to 40% were tested in an outdoor testing facility. The measured thermal performance showed that all the STPV windows possessed substantially larger heat gain coefficients than the normal reference glass. In addition, the heat losses were very large for these single pane STPV windows at night in winter. Both the high heat gain coefficients and large heat losses indicate that the overall thermal performance of single pane STPV windows is not satisfactory. According to the calculation results in WINDOW 7.2 software, the heat gain

and the U-value of a typical single pane STPV module are 335 W/m^2 and $5.468 \text{ W / m}^2 \cdot \text{k}$, respectively, under the NFRC 100-2010 simulation conditions.

In addition, during BIPV operations the PV module temperature was very high due to its high sunlight absorptivity. Our own experimental data showed that the maximum temperature of a semi-transparent a-Si PV module installed on the south-facing facade could reach up to $60 \text{ }^\circ\text{C}$. Such a high surface temperature would result in serious thermal discomfort in the indoor room if single pane PV modules were to be directly used as building facades. In addition, the heat losses through a single skin STPV window are very serious in winter nights due to its high thermal emissivity and U-value. In fact, the surface temperature of the STPV window was lower than the ambient temperature by about $2 \text{ }^\circ\text{C}$ at night due to infrared radiation to the night sky. The high U-value of single skin STPV windows would severely restrict their applications in cold climates. In order to reduce the thermal discomfort experienced as well as the severe heat losses, an optimized prototype should be developed which overcomes the overheating problem in summer and the severe heat losses in winter. A conventional insulating glass unit would provide some improvement year round but it is possible to provide even better performance. Thus, a novel naturally ventilated photovoltaic double-skin facade (PV-DSF) was developed by the authors to improve the annual thermal performance [25-26]. The ventilation design of the PV-DSF removes much of the waste heat generated during the PV module energy conversion processes in summer and thus also bringing down the operating temperature of the solar cells, further improving their energy conversion efficiency.

A literature research revealed that most of the research related to STPV windows/facades focused on thermal performance, such as solar heat gain coefficients

(SHGC), heat losses, the impact on the air-conditioning cooling load reduction and energy saving potential. A few researchers paid attention to daylighting performance, such as daylighting illuminance distribution and artificial lighting energy saving. It appears that no research regarding dynamic power generation performance has been reported. However, the power generation ability is surely one of the most important functions of STPV windows, a research gap requiring attention so as to comprehensively evaluate the overall energy performance. In addition, previous studies simulated the thermal effects, daylighting and power performances of STPV windows separately. But these factors are not independent of each other; since the performance of one affects the performance of the others. The optical characteristics at each wavelength not only determine the daylighting properties of STPV windows, but also significantly affect the thermal performance, the PV module's temperature as well as the power output performance. For example, if the transmittance of the semi-transparent PV module increases, the daylighting illuminance and the solar heat gain will go up, but the power output will decline. Similarly, if the absorptivity of the PV module increases, the module's temperature and the power output will go up, but the daylighting illuminance and solar heat gain may decline. Thus, a comprehensive simulation model is called for which can simulate the performances of all these factors simultaneously and hence calculate a more realistic overall energy performance.

In this paper, a simulation model was developed based on EnergyPlus to simulate the overall energy performance of a naturally ventilated PV-DSF. The interactions among thermal, power and daylighting performances were reasonably well modelled by coupling the energy balance model, heat transfer model, PV power generation model and optical

characteristics in EnergyPlus. EnergyPlus, as one of the most popular building energy simulation programs, can model the heat transfer, daylighting performance and PV systems simultaneously and deal with the interaction effects of thermal, power and daylighting based on fundamental energy balance principles. The optical characteristics (including absorptivity, reflectance and transmittance at each wavelength), heat conductivity and infrared emissivity of the PV module were measured and then inputted into the heat transfer model, WINDOW module and daylighting model for calculating the coupled thermal behavior and daylighting properties. The Sandia PV power model, also known as SAPM model, which takes into account the impacts of several power performance factors, was adopted to predict the dynamic power output of PV-DSF under different weather conditions. Based on the simulation work, a methodology for modelling the overall energy performance of semi-transparent PV-DSFs was derived as reported below. These simulated values were then compared to measured data taken in a test bed that incorporated a near exact physical replica of the PV-DSF system that was modeled in EnergyPlus.

2. Methodology of the Simulation Work

The ventilated PV-DSF reported in our previous publications consisted of an outside layer of semi-transparent a-Si PV modules, an inner layer of an inward opening window and an air ventilation cavity between these two layers. For more information on this PV-DSF, refer to [25-26]. It is, in fact, challenging to study the overall energy performance of a PV-DSF because of the interacting effects between the different performances as outlined above. The first step in simulating the overall energy performance was to find or develop an appropriate tool, able to not only simulate the thermal and daylighting performances of glazing double-skin facades but also predict the dynamic power output performance of

solar PV systems under different climate conditions. Given these required functions, EnergyPlus is a good choice [27].

In this study, in order to comprehensively investigate the overall energy performance of a PV-DSF, the PV power module, airflow network module, daylighting module as well as the WINDOW glass module in EnergyPlus were all utilized to simulate the power, thermal and daylighting performances, respectively. The schematic diagram of the simulation methodology is shown in Figure 1. The methodology and procedure are as follows:

- (1) The simulation work started by measuring the physical characteristics of the semi-transparent a-Si PV module, including its optical characteristics, infrared thermal emissivity and thermal conductivity.
- (2) The measured physical characteristics were input to Optics¹ for the creation of a physical characteristics file (with .mdb suffix) for the PV laminate.
- (3) The created .mdb file was then imported into WINDOW to add the PV laminate physical characteristics data to the International glazing database (IGDB).
- (4) A file with .IDF suffix was created by WINDOW and then imported into EnergyPlus together with the geometric dimensions of the PV-DSF and a customized weather data file to create the complete PV-DSF model. The customized weather data file was created using the measured weather data recorded by the team's own weather station which was located close to the outdoor PV-DSF test bed.

¹ Optics is a specific software for analyzing optical properties of multilayer glazing systems.

- (5) The EnergyPlus simulation manager employed modules and sub-models, such as the airflow network module, daylighting control model, sky model module, heat transfer model, Sandia PV power model, and others, to simulate the hourly overall energy performance of the PV-DSF, including power, thermal and daylighting performances.
- (6) The solar radiation model in EnergyPlus firstly converted the hourly horizontal solar radiations into plane of incidence irradiance; then the heat transfer model together with the airflow network model calculated the hourly temperatures and heat fluxes at each zone based on the ambient temperature, wind speed, incident solar radiation, building materials' physical characteristics and so on; lastly the daylighting model and the Sandia PV model were used to simulated the hourly daylighting illuminance and power output, respectively, based on the calculated plane of incidence irradiance. As the weather data is hourly basis in EnergyPlus, all the simulation results above are hourly values.
- (7) Many coefficients determined from indoor and outdoor tests were input to the Sandia PV power model to predict the PV-DSF dynamic power output under different weather conditions.
- (8) The accuracy of the comprehensive model developed was validated by comparing the simulated results with experimental data. Modifications were then made based on the comparison results to calibrate and improve this model.

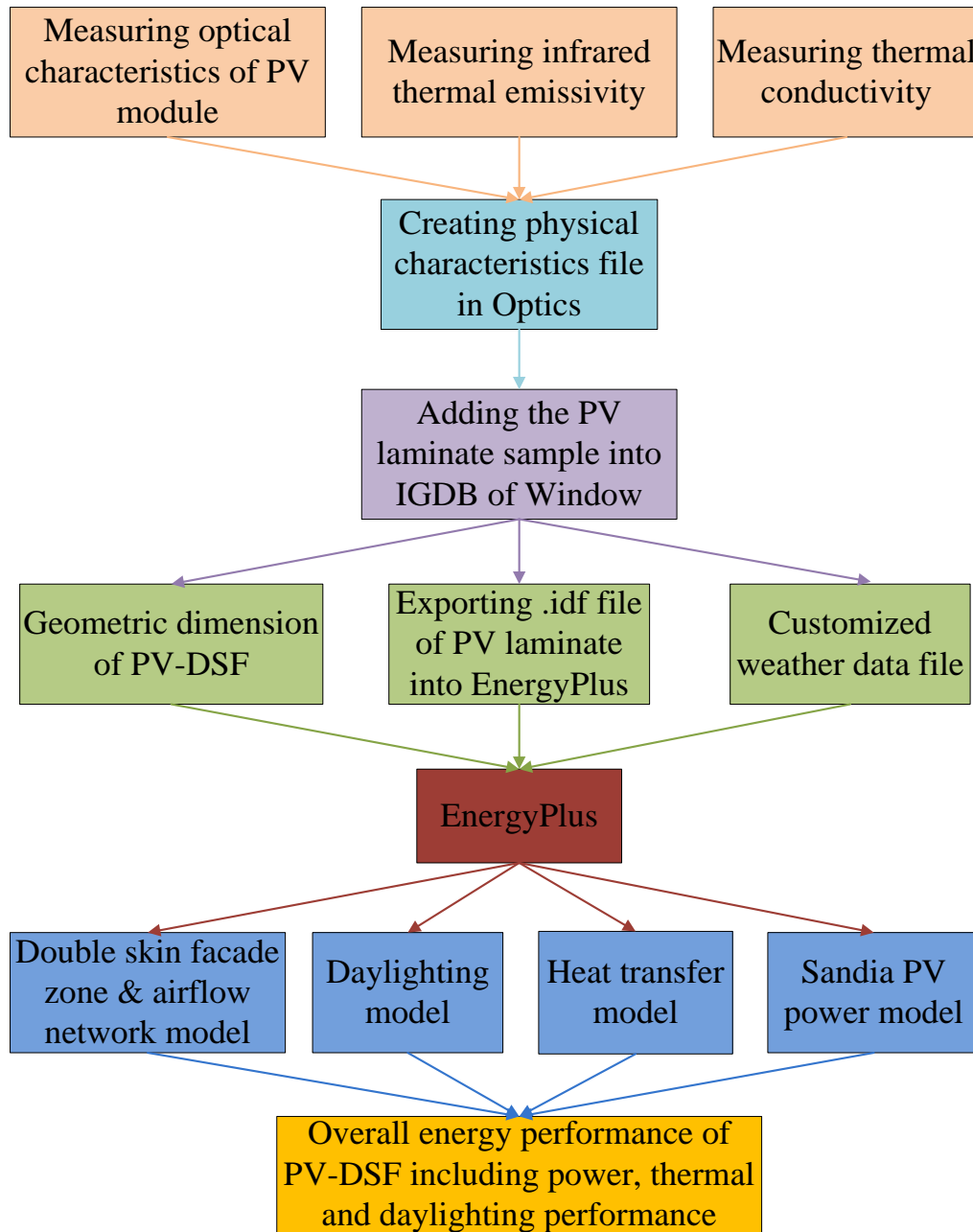


Figure 1. Schematic diagram of the simulation methodology for the PV-DSF

3. Measuring the Physical Characteristics

3.1 Optical Characteristics

The optical characteristics of the semi-transparent a-Si PV sample were measured using a spectrometer in the Optical Lab of Lawrence Berkeley National Laboratory

(LBNL). A Lambda 950 UV/VIS Spectrometer made by PerkinElmer was employed in the test. This machine can directly measure the diffuse transmittance (T_{diffuse}), total transmittance (T_{total}), diffuse reflectance (R_{diffuse}) and total reflectance (R_{total}) of the PV sample at each wavelengths from 300 nm to 2500 nm. The absorption of the PV sample can easily be calculated using Eq. (1):

$$\rho + \tau + \alpha = 1 \quad (1)$$

where, ρ is the reflectance, τ is the transmittance, and α is the absorption .

Figure 2 presents the photo of the semi-transparent a-Si sample used for measuring. This PV module was fabricated by Bosch Solar Energy. It was a sandwich structure, consisting of a 3 mm transparent conducting oxide (TCO) glass on which the a-Si layers (P-I-N) were deposited, a polyvinyl butyral (PVB) layer and a 3 mm rear glass. Lastly, the sandwich-type PV module was formed in a hot press molding machine. Figure 3 presents the optical characteristics of the semi-transparent a-Si PV sample. The average values of R_{diffuse} , R_{total} , T_{total} and T_{diffuse} were 0.035, 0.115, 0.213 and 0.006, respectively integrated across the total solar spectrum. The average transmittance in the visible light range was about 7%, which is relatively low for building occupants having a good outside view. However, four years ago, when the PV-DSF was built, the efficiency of normal a-Si PV modules was relatively low, less than 7%, thus a tradeoff between the power and daylighting performances must be effected at that time to maximize the energy benefits for this kind of PV-DSF. Obviously, a higher PV module transmittance would result in a decline of energy conversion efficiency as well as an increase of solar heat gain coefficient (SHGC). With this in mind, the semi-transparent PV modules with 7% transmittance rather than 20% transmittance were chosen for the PV-DSF because of its better power performance, solar control performances

together with an acceptable daylighting performance since the façade was fully glazed. Its energy conversion efficiency was 6.2% under the standard testing conditions (STC). From the view point of daylighting, 7% transmittance is relatively low, but it does not affect the study on daylighting performance. The model developed based on the 7% transmittance PV module in this study should be also suitable for PV modules with different transmittances.



Figure 2. Photo of the semi-transparent a-Si sample used in this study

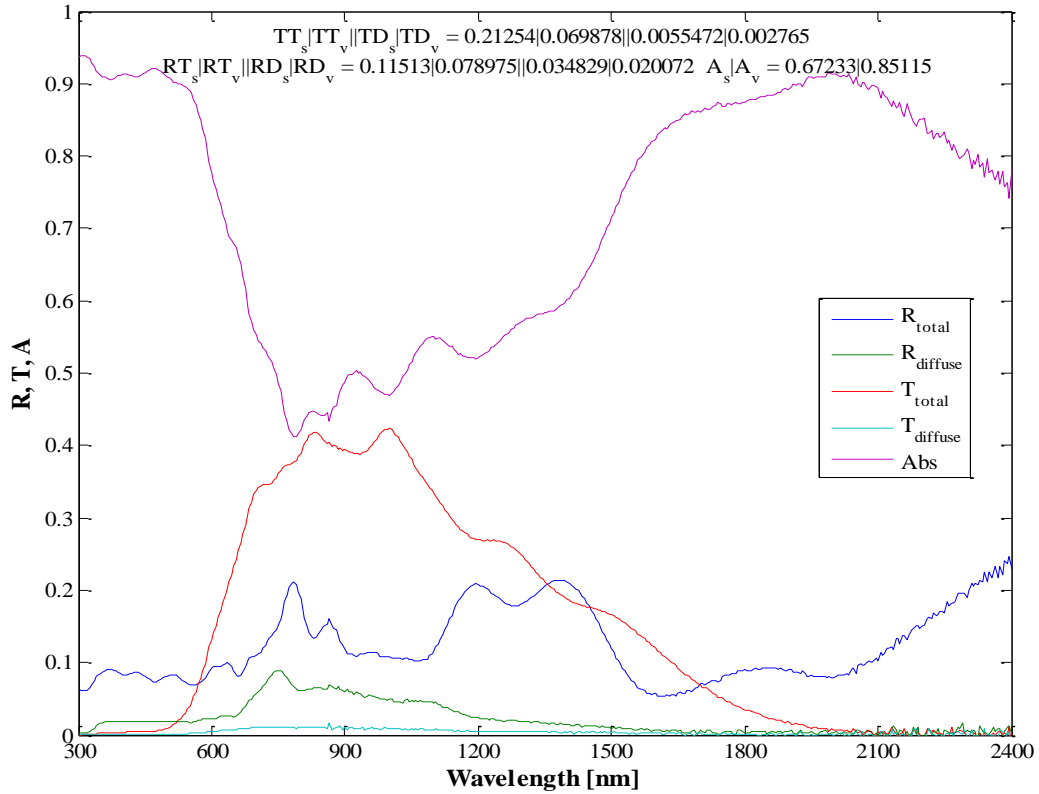


Figure 3. Optical characteristics of the semi-transparent PV Sample

Nowadays, with the efficiency of a-Si PV modules increasing, a series of semi-transparent PV modules with high transmittance (20% or larger) are emerging, whose efficiency are not less than 6.5%. As shown in Figure 4, when the transmittance increases to 20%, the visual effect of the PV module is improved significantly. Even though it is impossible to compare with normal glazing windows in terms of view, it is acceptable considering its energy benefits for occupants, its energy conversion efficiency was 6.7% under STC.



Figure 4. Visual effect of a a-Si PV module with 20% transmittance
(from inside to outside)

3.2 The Infrared Emittance and Thermal Conductivity

Infrared emittance is an important parameter related to the thermal insulation performance of PV modules as it affects the heat loss and U-value considerably. The larger the infrared emittance, the larger the heat loss and U-value, such that the thermal insulation performance of the PV module is worse. As shown in Figure 5, the front and rear emittances of the PV sample were measured by an emissometer made by Devices and Services Co. This emissometer, combining with a scaling digital voltmeter, is a special purpose instrument for measuring emittance [28]. Its accuracy and repeatability is ± 0.01 . The test results showed that the front and rear emittances of the PV sample were 0.85 and 0.83, respectively, which are consistent with the exposed glass surfaces of the laminate construction where the amorphous PV layers is protected within the laminated glazing.

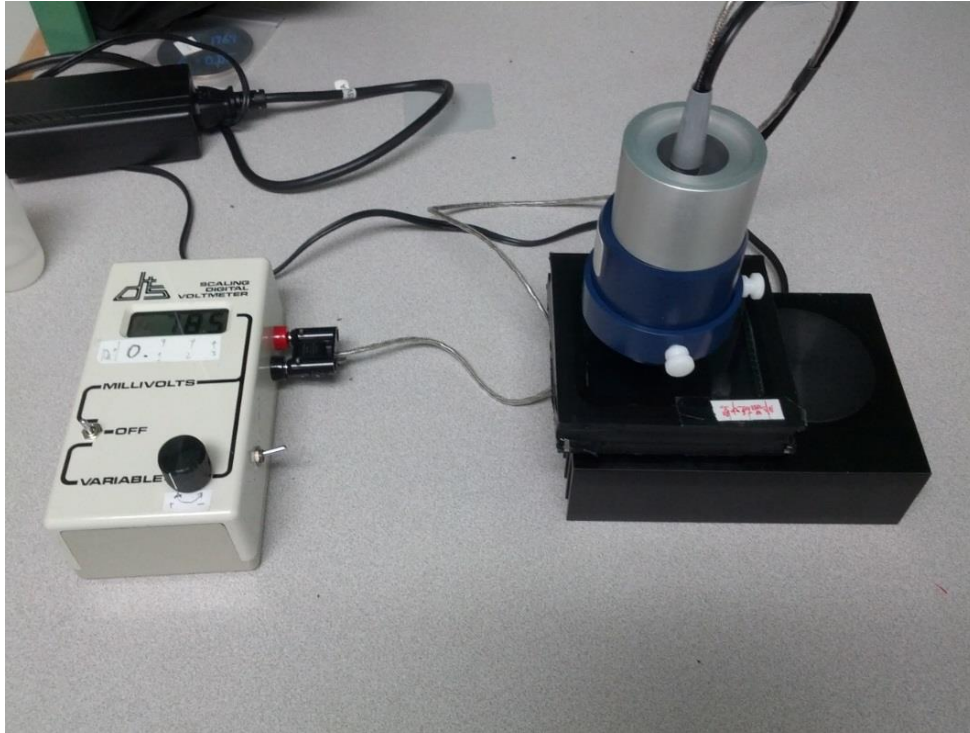


Figure 5. Measurement of infrared emittances for the PV sample

The other important thermal performance parameter is thermal conductivity. The thermal conductivity of the PV sample was measured by an instrument made by the LaserComp Co., as shown in Figure 6. This instrument can precisely measure the thermal conductivity of objects subjecting to different temperature differences by combining with a refrigerating unit. The absolute thermal conductivity accuracy is $\pm 2\%$ in the temperature range $-20^{\circ}\text{C}\sim 75^{\circ}\text{C}$, and the reproducibility is $\pm 0.5\%$. In this test, the front of the PV module was heated to 55°C while the rear was cooled to 30°C , and the temperature difference between the two sides was kept at 25°C , which is representative of the real temperature difference of such a PV module if operational on a real building. The measured thermal conductivity under this temperature difference condition was $0.48\pm 0.01\text{ W}/(\text{m}\cdot\text{K})$.



Figure 6. Measurement of the thermal conductivity of the PV sample

3.3 Inputting Physical Characteristics

Using the measured physical parameters of the PV module the next step was to input these measured data into Optics to create a physical parameter file (with suffix .mdb), which can be recognized and compiled by WINDOW. WINDOW is a professional software program which can be used to calculate the overall thermal and solar optical properties of glazing and window systems based on their components [29]. Optics is a specific software program for analyzing and processing the optical properties of multilayer glazing systems. It can generate an accurate full spectral data set for various glazing systems. The .mdb file exported from Optics was then imported into WINDOW for creating a spectral data file for the PV module (with suffix .IDF).

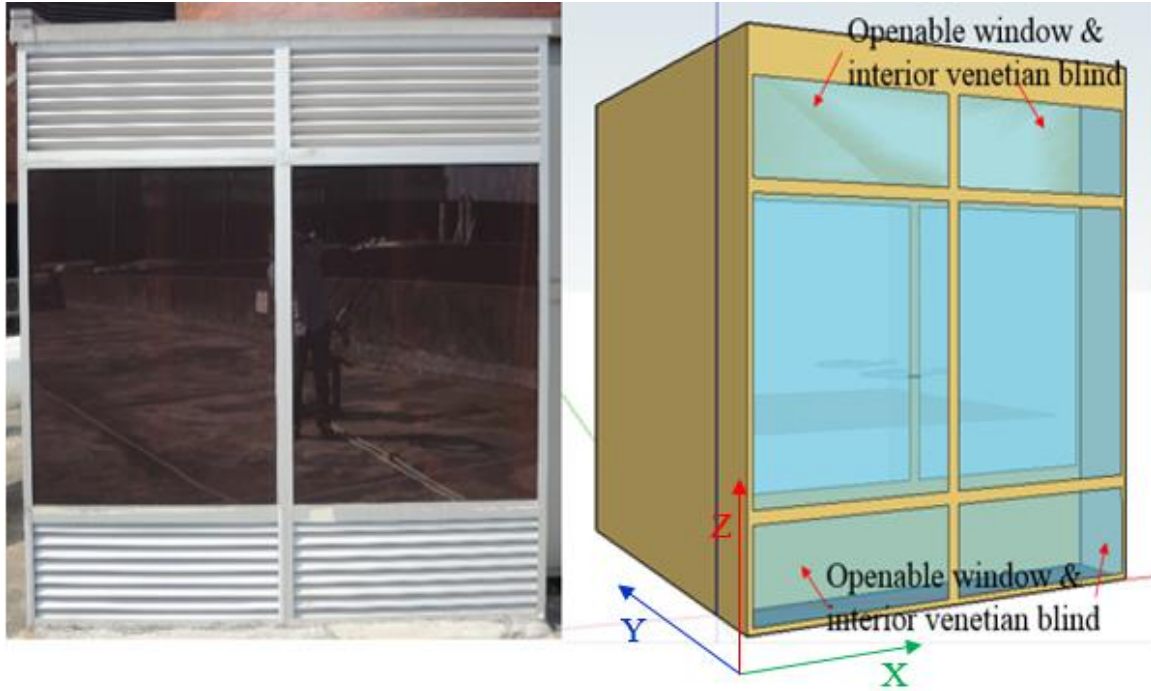
4. Modeling in EnergyPlus

4.1 Creating a PV-DSF Test Bed Model

Besides the PV module spectral data (.IDF file), the geometric dimensions of the PV-DSF and a customized weather data file also need to be imported into EnergyPlus. Table 1 gives the key dimensions of the PV-DSF test bed. Figure 7 compares the real PV-DSF test bed with the PV-DSF model in EnergyPlus.

Table 1 Key dimension parameters of the PV-DSF model

Parameters	Value
Width of the office room	2.32 m
Depth of the office room	2.3 m
Height of the office room	2.5 m
Width of PV module	1.1 m
Height of PV module	1.3 m
Thickness of PV module	0.008 m
Width of louver	1.1 m
Height of louver	0.45 m
Depth of air flow cavity	0.4 m
Window wall ratio	0.6



(a) The real PV-DSF test bed (b) The simulation model in EenergyPlus

Figure 7. Comparison of the real PV-DSF and the PV-DSF model in EnergyPlus

With respect to the geometric dimensions and wall materials, the simulation model was identical to the real PV-DSF. The glass IDs of the openable windows and the internal windows of the PV-DSF chosen in the simulation were NFRC (National Fenestration Rating Council) 411 and NFRC 412, respectively, which were coincided with the real glasses adopted in the PV-DSF test bed. Table 2 presents the key physical properties of these two kinds of glasses. The wall chosen in the simulation model were also similar with that of the real PV-DSF test bed. It was a sandwich structure wall, and its thermal properties are presented in Table 3.

Table 2 Key physical properties of the glasses used

Glass ID	NFRC 411	NFRC 412
Glass type	Clear float glass	Clear float glass

Thickness (mm)	2.24	3.0
Transmittance of visible	0.9	0.9
Transmittance of solar light	0.856	0.838
Emissivity	0.84	0.84
Thermal conductivity	1	1

Table 3 Thermal properties of the wall

Items	Wall
Materials	Steel sheet (1.59 mm)+ Expanded Polystyrene (48.3 mm)+ Steel sheet (1.59 mm)
Thickness (mm)	51
U-factor (W/m ² /k)	0.62
R-value (m ² /k/W)	1.60

The only difference between the real PV-DSF and the simulation model was that four openable windows with interior venetian blinds were adopted for the simulation model to replace the inlet and outlet louvers of the real PV-DSF because EnergyPlus cannot model louver components. The four openable windows were kept fully open during the whole simulation process and the interior venetian blinds which are not shown in Figure 7(b) were assumed similar in effect to the louvers of the real PV-DSF. Although no direct experimental data can be used to support the assumption for the louver component, its reasonability has been indirectly validated later through comparing the simulation results of PV module temperatures, daylighting illuminance and heat gains with the measured data. As the simulation results needed to be validated against experimental data, a customized weather data file was created based on measured weather data in the winter of 2012 -2013 (from October to March), recorded at the weather station located in the campus of the Hong Kong Polytechnic University, nearby to the PV-DSF test bed location. The gathering time

of weather data was coincide with the period of outdoor experimental campaign, such that the simulation results can be validated with the experimental data with the same weather boundary conditions. This weather station, every minute, can measure and record air temperature, relative humidity, precipitation, horizontal global solar radiation, horizontal diffuse solar radiation, direct normal irradiance, wind speed and direction. The customized weather data file was imported into EnergyPlus as boundary conditions to validate the simulation results.

EnergyPlus includes and integrates many modules and models to simulate heat and mass transfer, daylighting performance, on-site renewable energy power output as well as building systems [27]. In order to simulate the ventilation effect of PV-DSF, the airflow network model and heat transfer model were made use of in this study. The daylighting model in EnergyPlus was chosen to simulate the daylighting performance under different weather conditions as well as the corresponding saving in artificial lighting energy. For the PV power output, the Sandia PV power model was chosen to simulate the hourly dynamic power output under arbitrary weather conditions.

4.2 Airflow Network Model

One of the important advantages of the ventilated PV-DSF is that the airflow in the ventilation cavity between the external PV modules and the internal normal windows can not only bring down PV module operating temperatures but also reduce heat transfer between the indoor room and the outside. This ventilation cavity was represented by an independent zone named “Double-skin facade zone” in the simulation model in EnergyPlus, as shown in Figure 8. In order to accurately simulate the impacts of ventilation on the power performance improvement and on the cooling load reduction, the Airflow Network

model was used to simulate the heat transfer and air flow in the ventilation cavity. The Airflow Network model is able to simulate multi-zone airflows driven by outdoor wind, buoyancy and forced air [27]. Two nodes were defined in the simulation, as shown in Figure 8, they were located in the middle of the inlet and the out let louvers, respectively. The calculation flowchart of the Airflow Network model is given in Figure 9. Firstly, the pressure at each node and the airflow through each linkage are determined by the pressure and airflow calculations taking into account of the wind pressures and forced airflows. To take account of the opening louvers in this study, the “Airflow Network: Multizone: Component: Detailed Opening” was chosen to simulate the relationship between airflow and pressure in the ventilation cavity. Using the calculated airflow for each linkage in the previous step, the Airflow Network model then calculated the node temperatures and humidity ratios with the given zone air temperatures and zone humidity ratios. Based on the node temperatures and humidity ratios calculated in the second step, the sensible and latent loads were summed for the cavity. Finally, the final zone air temperatures, pressures and humidity ratios were determined. Thus, as mentioned above, the Airflow Network model successfully simulated the airflow rate and temperature distribution in the PV-DSF cavity. These data were then used to calculate the resultant impacts on the room cooling loads from solar heat gain and conduction through the inner glazing. The room cooling loads mainly derived from the heat flux through the PV-DSF and the sandwich-structure walls as well as the heat-producing of the data acquisition system.

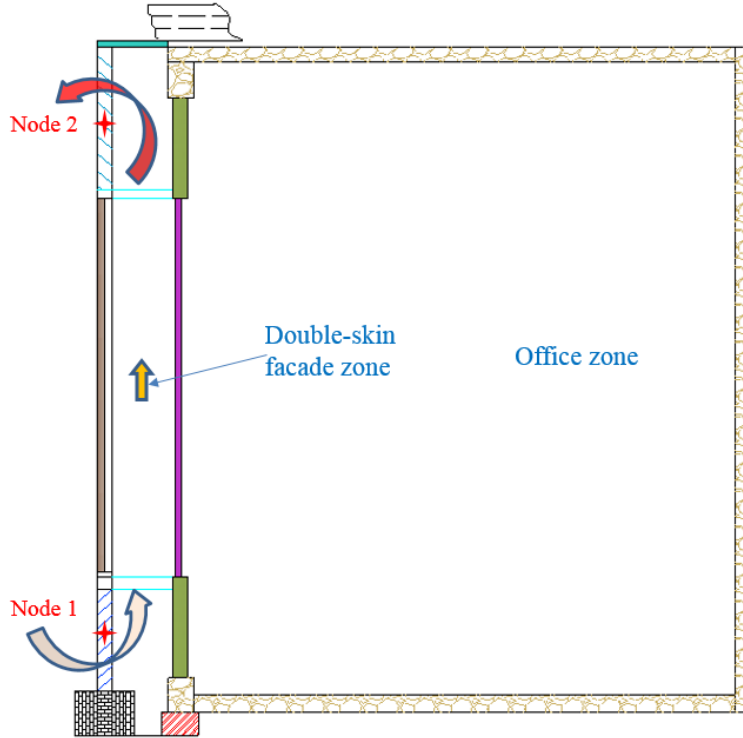


Figure 8. The defined double-skin facade zone in the PV-DSF model

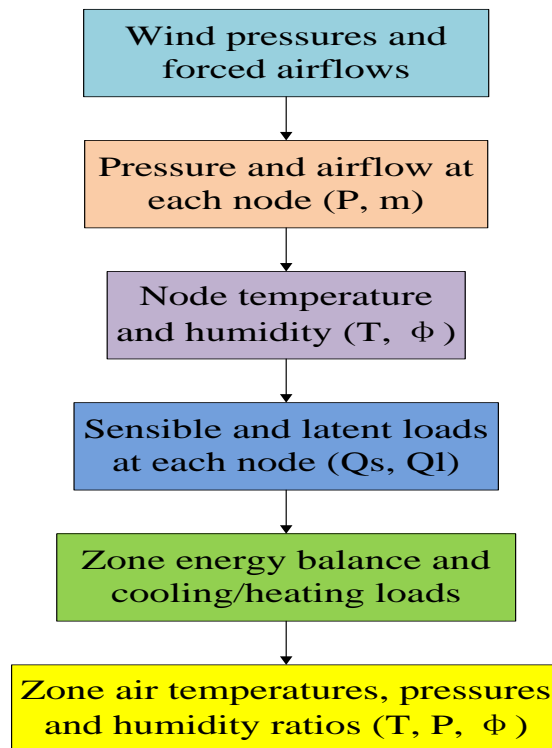


Figure 9. Calculation flowchart of the Airflow Network model

4.3 Daylighting Model

The PV modules adopted in the PV-DSF were semi-transparent, and the transmittance was about 7% in the visible light range. Thus, some daylight could penetrate the PV-DSF and enter the indoor room. In addition, natural lighting was able to pass through the slat gaps of the upper louver and enter the workspace, improving the daylighting performance significantly. The upper louver's dimensions were 1.1×0.45 m (W×H). It had 5 slats which were fixed with 20 degree to the vertical. According to the simulation results, the lighting energy use of the room equipped with the PV-DSF could be reduced by about 11% if combined with an automatic dimmable lighting system,

In this section, the Daylighting model in EnergyPlus was used to simulate the PV-DSF daylighting performance as well as the impact on light energy usage for different weather and sky conditions. Figure 10 presents the flowchart of the simulation of daylighting performance. Firstly, the user specifies the lighting reference point coordinates in the daylighting zone. In this study, a reference point was specified with X, Y, Z coordinates of (1.3 m, 1.1 m, 1 m). As shown in Figure 7 (b), the origin of the coordinates was located at the left bottom of the model, and X axis is in reference to the width along the PV-DSF, Y is in reference to the distance from the inner glazing window, Z is the height from the floor. Then, the exterior horizontal illuminances due to sky-related light and sun-related light under standard sky conditions, such as clear sky, clear turbid sky, intermediate sky and overcast sky, were calculated and stored. The exterior horizontal illuminance due to diffuse radiation from the sky was calculated for each of the above four sky conditions by integrating over the appropriate sky luminance distribution. The actual exterior horizontal illuminance due to beam solar irradiance was determined by combining

the direct normal solar irradiance from the weather data file and the empirically determined luminous efficacy in the time-step calculation [27]. The interior daylighting illuminance consists of the two components, viz. direct component from a particular window and internally-reflected component from the interior ceiling, floor and wall surfaces. The direct component of daylight illuminance at a reference point due to a particular window was determined by dividing the window into an x-y grid and then finding the flux reaching the reference point from each grid element. The internally-reflected daylighting illuminance component reaching a reference point can be calculated by using the split-flux method [30-31].

After calculating the corresponding interior daylighting illuminance, the daylight factors of the PV-DSF under standard sky conditions and representative sun positions were deduced by dividing the interior illuminance by the exterior horizontal illuminance. The representative sun positions refer to hourly sun positions on the local sun-paths of representative days for a given geographical location. Based on the Sun position of the current time step and sky conditions, the current daylight factor was found by interpolating between the representative daylight factors calculated in the previous step. At the same time, the current exterior horizontal illuminance was calculated from the current solar irradiances and solar zenith angle. The daylighting illuminance level at the reference points were then obtained by multiplying the current daylight factors with the current exterior horizontal illuminance. Comparing with the design illuminance level, if the daylighting illuminance did not meet the design requirements, the artificial lighting would make up the gap and the corresponding required amount of electricity for lighting was also calculated. As the required amount of lighting electricity reduced, so the cooling load due to that

artificial lighting would also reduce. Thus, the better the daylighting utilization the more the reduction in lighting electricity and the more the reduction in cooling loads, because natural light has a higher luminous efficacy (lm/W) than artificial lighting [32-33].

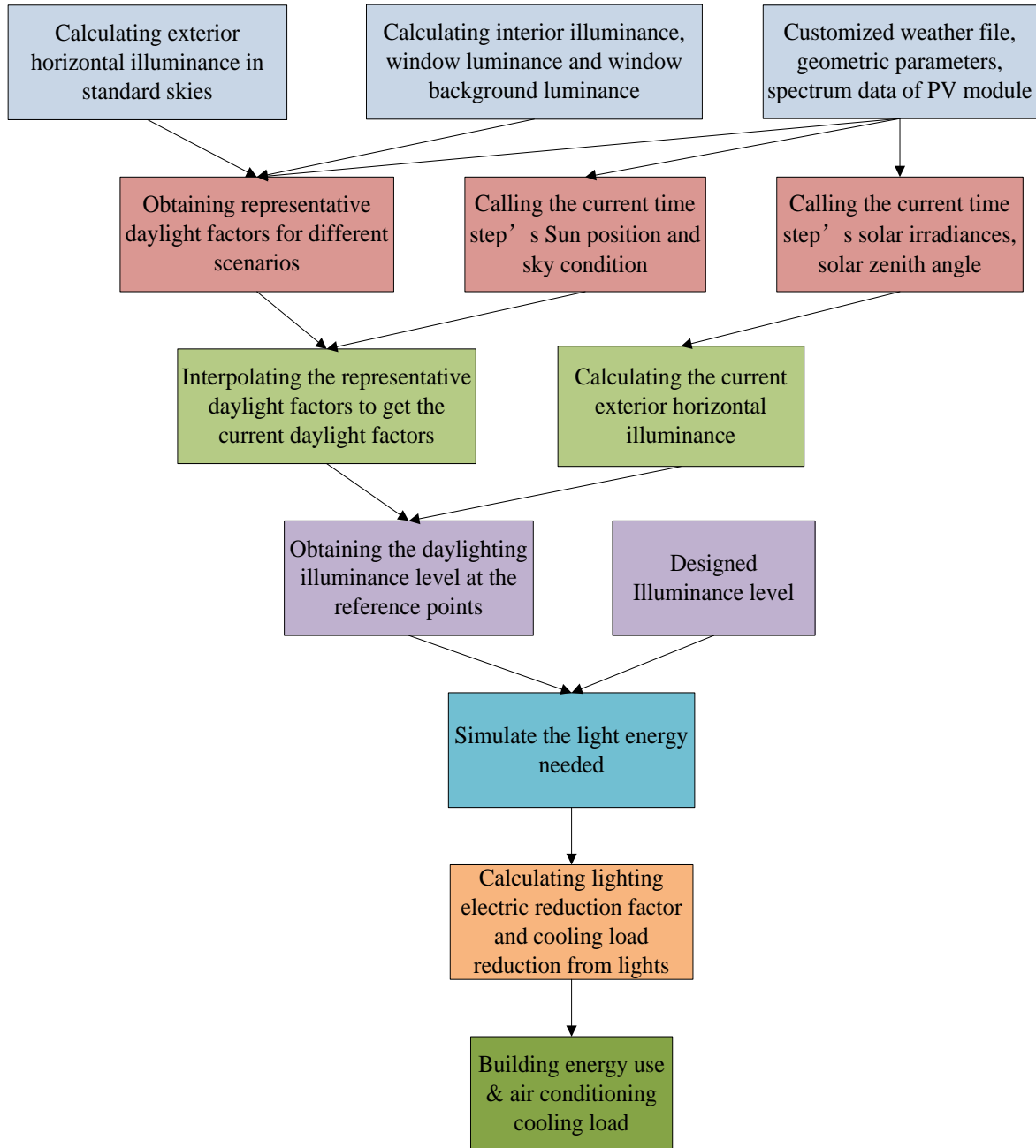


Figure 10. Flowchart of simulating the daylighting performance of PV-DSF

4.4 PV Power Model

The main reason for choosing EnergyPlus to simulate the overall energy performance of the PV-DSF is that not only it can simulate the thermal performance and daylighting performance of glazing facades but also predict the on-site power generation of renewable energy installations, especially for building-integrated photovoltaic systems (BIPV). EnergyPlus integrates three different PV power simulation models, “Simple model”, “equivalent one-diode model” and “Sandia model” [27]. All the three models share the same solar simulation model for calculating the incident solar irradiation. The differences lie in the processes of simulating the PV power output at the same solar irradiation. The Sandia model, also known as the Sandia Array Performance Model (SAPM), is empirically based, and achieve versatility and accuracy for almost all PV technologies, especially for thin-film solar cells, because the coefficients used in this model are derived from special tests with the same kind of solar cell [34]. Before using this model, users have to carry out many special tests to obtain a series of coefficients for their PV module to be simulated. However, once the coefficients required by the model are obtained, it can accurately simulate the power output of the PV module for all arbitrary weather conditions because this model considers the impacts of many factors on the power performance, such as solar incident angle, operating temperature, solar spectrum distribution and so on [35-36]. Thus, the SAPM was chosen in this study for prediction of hourly dynamic power output performance of the a-Si PV-DSF.

The fundamental equations of the SAPM can be found in [34]. To solve these fundamental equations, values of 39 parameters in total have to be input into the SAPM in EnergyPlus for predicting PV module power output performance. Except for 3 parameters

which can be obtained easily, 36 parameters had to be specially measured or fitted from curves. In previous studies, almost all the parameters, including the electrical characteristics under standard test conditions (STC) and the temperature coefficients, were measured outdoors [34, 37]. However, as the outdoor weather conditions are uncontrollable and rarely close to the STC conditions (1000 W/m² solar radiation, 25 °C, AM 1.5), the outdoor testing process is complicated and time-consuming. Thus, based on the previous studies, a set of simple indoor and outdoor measurement methods was developed to determine the empirical coefficients of the SAPM for semi-transparent a-Si PV modules [38]. Actually, about half of the SAPM coefficients were extracted from indoor measurements using a solar simulator in this study, while the other coefficients, such as the coefficients of the solar spectral correction function, were derived from outdoor measurements. To correct the impact of angle of incidence (AOI) on the power performance, a polynomial function developed in [34] was used in this study to modify the hourly short circuit current under different incident angles. When all 39 parameters of the SAPM were determined, the PV module's dynamic power output could be predicted, knowing also the instantaneous incident solar irradiance, operating temperature and air mass. Five key points on the I-V curve were determined based on the fundamental equations and the I-V curve itself was then fitted according to these five points. Figure 11 presents the five key points and the I-V curve for the a-Si PV module studied under standard testing conditions (STC). Point A is the maximum power point of the PV module under STC.

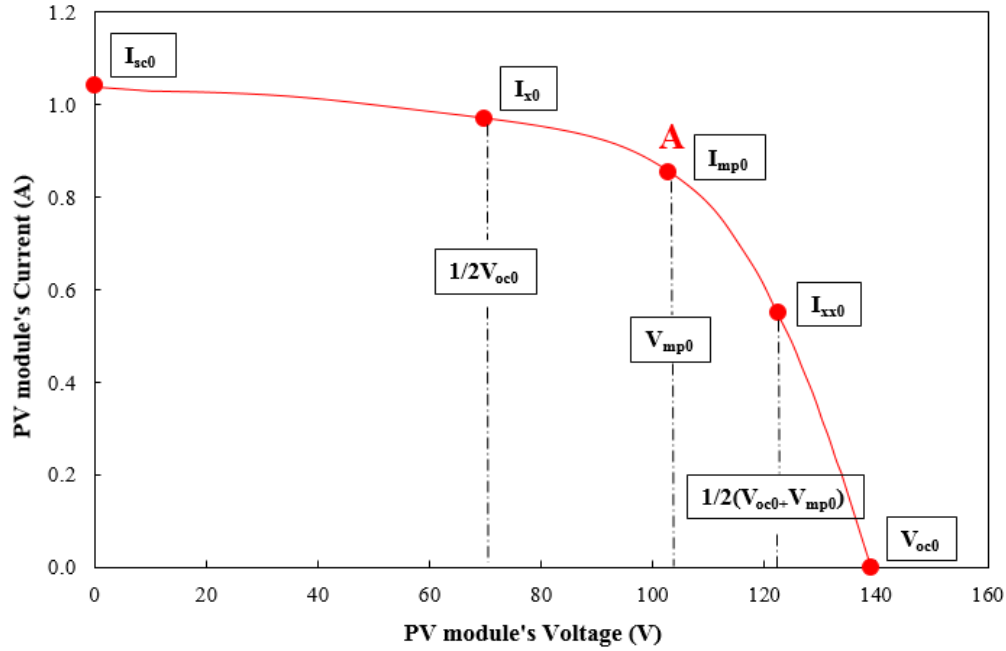


Figure 11. I-V curve and its five key points of the a-Si PV module under STC

The last step was to consider the impact of power generation on the heat transfer balance of the PV module. Unlike a normal glass window, as some part of the solar energy is converted into electricity, the heat transfer balance as well as PV module temperature distribution was changed for the PV-DSF. EnergyPlus provides different heat transfer modes enabling the SAPM to achieve coupling between energy generation and heat transfer. The “Integrated Surface Outside Face” mode was used in this study, whence, the solar cell temperature refers to the outside face temperature of the PV module. When calculating the heat transfer and temperature distribution, the energy generated by the PV module was removed from the heat transfer balance equations. Thus, the interaction effects between the power performance and thermal performance were reasonably well represented.

5. Model Validation

The PV-DSF model developed was then validated against experimental data to verify its accuracy. The outdoor experimental campaign was carried out in the winter of 2012-2013, from October 1 to March 10. Much of the data gathered during the outdoor testing of the real PV-DSF were available for model validation, such as the PV module temperature, inside window heat gain, indoor daylighting illuminance and the power output.

5.1 Introduce to the PV-DSF Test Bed

A real PV-DSF test bed was built in the campus of the Hong Kong Polytechnic University to test its overall energy performance under real outdoor environment. Figures 12 and 13 present the schematic diagram and a real picture of the PV-DSF test bed, respectively. The weather station, made by Thies Clima, measured and recorded the local wind speed and direction, the ambient air temperature and humidity, as well as the horizontal global and diffuse solar irradiances. The solar irradiances were measured by two pyranometers installed on a sun tracker, as shown in Figure 13, which can track the sun from sunrise to sunset. As for the power generation, the DC power generated by the PV-DSF was firstly converted into AC power by micro-inverters, and then the AC power was transferred into the main distribution box. The DC and AC power output of the PV-DSF was measured by the micro-inverters and then transported to the computer via the communications gateway. The micro-inverter adopted is Involar MAC250B, which was a special inverter designed for thin-film PV modules with high open circuit voltage.

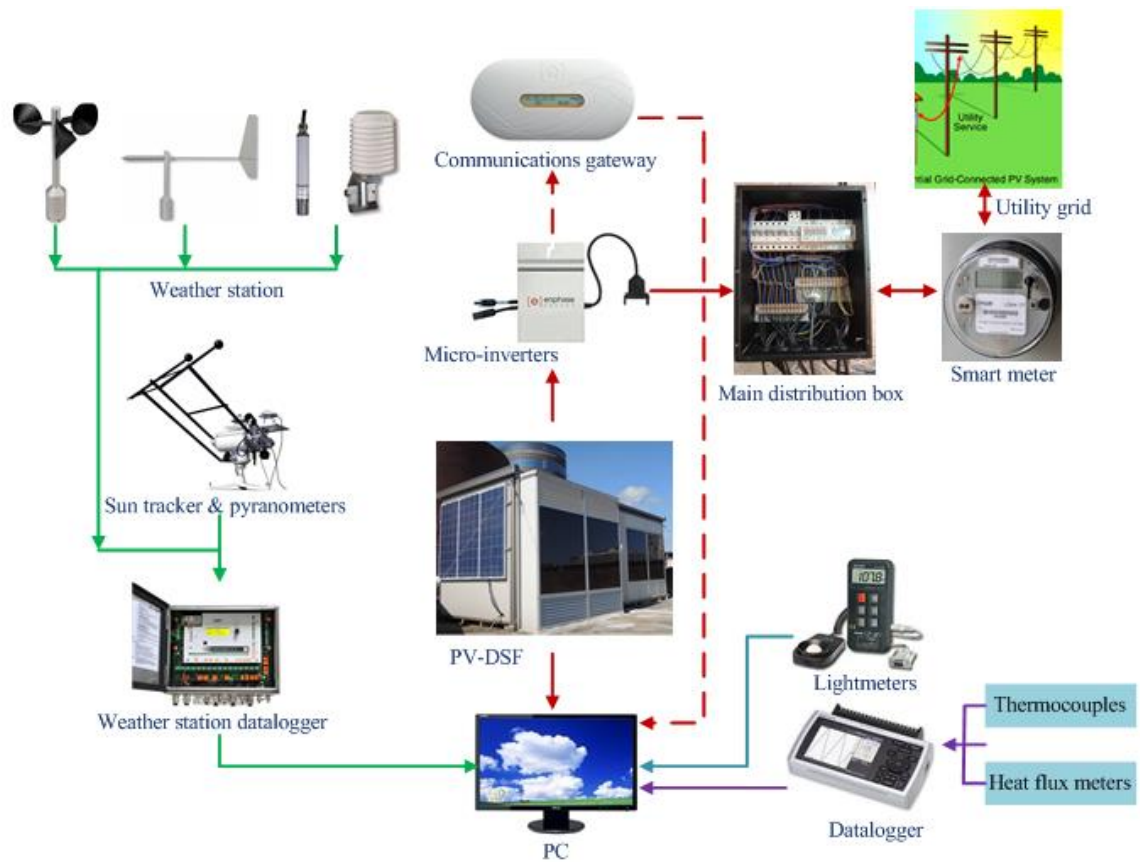


Figure 12. Schematic diagram of the PV-DSF test bed

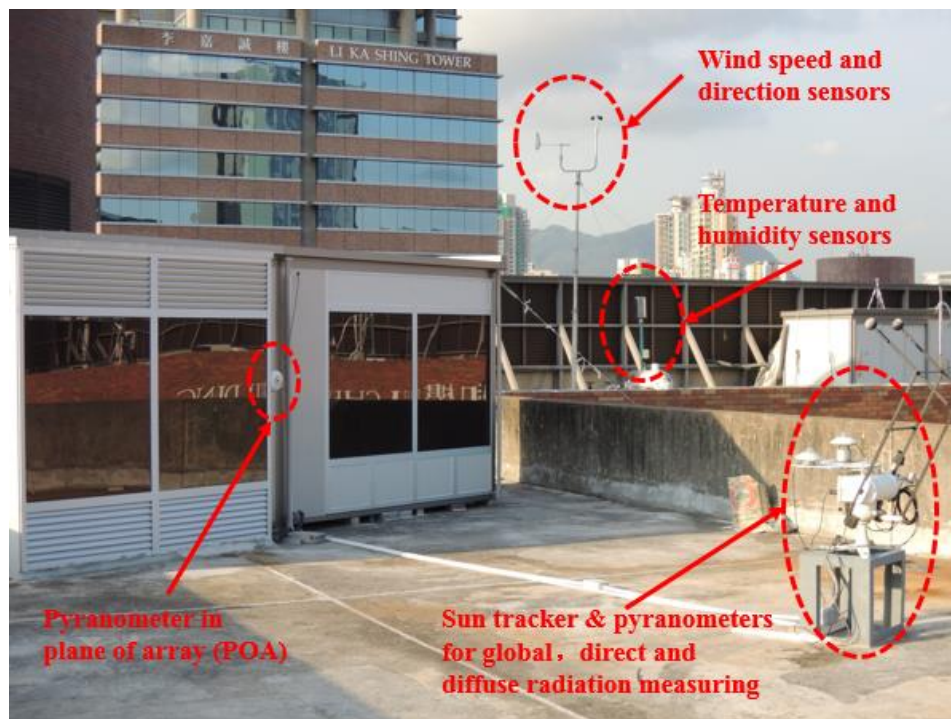


Figure 13. Picture of the PV-DSF used for outdoor experimental campaign

For the thermal performance, sensors, including thermocouples and heat flux meters, were installed on the ventilated PV-DSF to measure the temperatures in the air cavity and various surfaces, as well as the heat flux through the inside window. These sensors' signals were recorded by a GL820 Midi DataLogger, which can accept voltage (from 20mV to 50V), temperature, humidity, pulse and logic signals. During the experimental campaign, the indoor room temperature was conditioned by a split air conditioning and the design temperature was set to be 22 °C, which was the same as the setting temperature in the simulation model. To evaluate the daylighting performance of the PV-DSF, a light meter was placed horizontally in the middle of the room (coordinates: X, Y, Z: 1.3m, 1.1m, 1m), where had the same coordinates as the lighting reference point in the simulation.

All the above data or signals were recorded by the corresponding data loggers or professional software programs at a time interval of 1 minute during the testing campaign. The specifications and measurement uncertainty of the key instruments adopted are listed in Table 4. It is seen that the measurement uncertainties of most of instruments are less than 3%.

Table 4 The key experimental instruments and their specifications

Experimental Equipment	Manufacturer and model	Sensitivity and/or technical data	Measurement uncertainty
Weather station	Thies Clima	Wind speed: 0.1m/s; Wind direction: 1° ; Temperature: 0.1°C; Humidity:0.1%;	Nil

Pyranometers	EKO instruments (MS-802)	Sensitivity: about 7 $\mu\text{V}/(\text{W}/\text{m}^2)$;	Non-linearity < 0.2 % (at 1000W/m ²);
Thermocouples	RS components (T type thermocouple)	Temperature range: -200 ~ 350°C;	- 40°C < t < 120°C = $\pm 1.5^\circ\text{C}$;
Conductive heat flux meters	Captec Enterprise (HS-30)	Sensitivity: 2.5 $\mu\text{V}/(\text{W}/\text{m}^2)$; Response time: 0.3 seconds;	< 3%;
Data logger	Graphtec (GL820 Midi DataLogger)	Accepts Voltage (20mv to 50V), temperature, humidity, pulse and logic signals;	The minimum resolutions are 1 μV and 0.1 °C;
Light meter	TES (1336A)	Resolution: 0.01 Lux; Sensor: Silicon photo diode	$\pm (3\% \text{ rdg} + 5\text{dpts})$ (calibrated to standard incandescent lamp, 2856 K);
Micro-inverter	Involar (MAC250B)	Recommended Input Power (STC): 250W/200W~260W; DC voltage operating range: 60V~150V; MPPT Voltage Range: 72V~120V; Maximum DC Current: 3.47A	Power Factor > 0.99; Peak Inverter Efficiency: 94.5%; CEC Weighted Efficiency: 93.2%.

5.2 Validation of PV Module Temperatures

A comparison of the simulated solar cell temperature and the measured PV module back-surface temperature is presented in Figure 14. The measured PV module back-surface temperature is a little higher than the simulated solar cell temperature, and the back-surface

temperature at noon on sunny days, the maximum temperature difference was about 3 °C. On overcast days, the simulated temperatures coincided with the measured temperatures very well. The possible reasons causing the above cases were also analyzed. Firstly, although the environmental wind speed used in the simulation model was derived from the measured weather data, the airflow network model may overestimate the airflow velocity in the ventilation cavity and thus overestimate the convection heat transfer coefficient. Secondly, in the experiment, the thermocouple was attached at the middle-upper part of the PV module to measure the temperature there, however in the simulation model the PV module temperature was the average temperature of the whole PV module. On sunny days, under the effect of thermal buoyancy, the measured temperature at the upper part can be higher than the average temperature by 1-1.5 °C. Lastly, on sunny days, the reflected solar radiation from the concrete ground floor also resulted in the temperature rise of the PV module, but this impact was not effectively handled in the simulation model. The above reasons together may result in the case that the measured PV module temperature was higher than the simulated one at noon of sunny days.

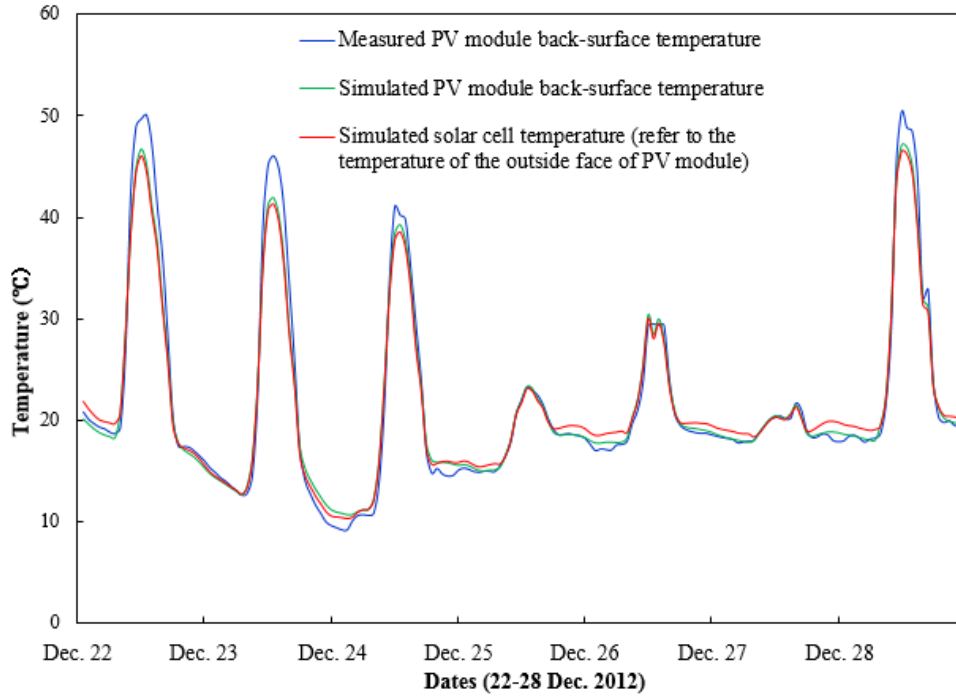


Figure 14. Comparison of the simulated solar cell temperatures and the measured PV module temperature

To quantify the errors between the simulated results and the experimental data, the mean absolute percentage error (MAPE) [39] was adopted in this paper. The MAPEs between the simulated PV module back-surface temperatures and the measured results on sunny days (from Dec. 22-24 and Dec.28) and overcast days (Dec.25-27) were 6% and 1.7%, respectively.

5.3 Validation of Daylighting Illuminance

A comparison of the simulated and measured indoor daylighting illuminances was also made. Figure 15 presents both sets of the simulated and measured daylighting illuminances at the lighting reference point 1. It is found that the indoor daylighting illuminance exceeded 300 lux and was close to 400 lux at noon on sunny days. This illuminance level meets the lighting requirements for many indoor activities [40], and it is

only lower than the design illuminance level for paper based work in Hong Kong by 100 lux [41]. Since the PV module's full wavelength-based spectrum data was used, the simulated daylighting illuminance at the reference point 1 (1.1 meters away from the inner window) agreed well with the measured data on sunny days, as shown in Figures 15, but the simulated daylighting illuminance deviated from the measured data on overcast days. The main reason causing the deviation of daylighting on overcast days was the rapid and strong fluctuation of solar radiation. In EnergyPlus, the daylighting illuminance was calculated based on the hourly solar radiation values of the TMY3 weather data file, however, the solar radiation fluctuates strongly and rapidly on overcast days, thus the hourly average solar radiation used for daylighting calculation could not accurately reflect the real sun and sky radiation conditions any more, thus the calculated daylighting illuminance is certainly different from the measured one. In contrast, on sunny days, the solar radiation increases/decreases gradually, the hourly average solar radiation can represent the sun and sky radiation conditions in this period, thus the calculated daylighting illuminance coincide with the measured data better. The MAPEs between the simulated and the measured daylighting illuminance on sunny days (Oct. 20-25) and overcast day (Oct. 26) were 8.3% and 14.4%, respectively.

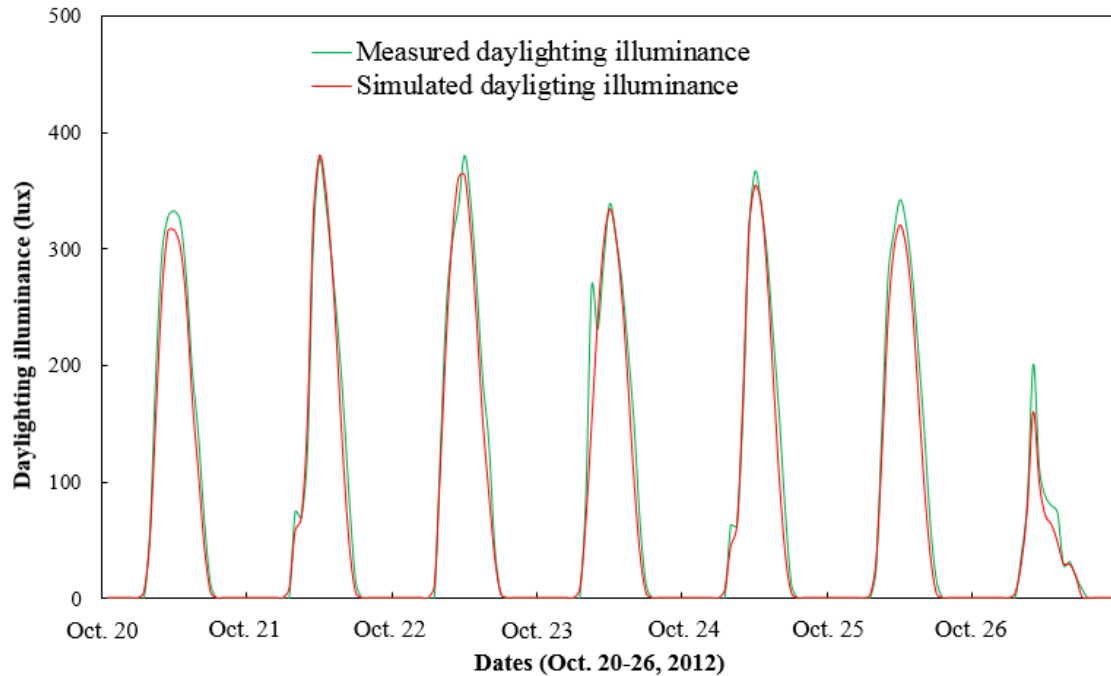


Figure 15. Comparison of the simulated daylighting illuminance and the measured one

To quantify the impact of daylighting on the power consumption of artificial lighting, a term of lighting energy use was introduced, which was defined as the energy used by artificial lighting to meet the design illuminance level. The lighting energy use under different daylighting illuminance levels were also simulated in this study to demonstrate the impact of daylighting on the energy use of artificial lighting. As shown in Figures 16 and 17, with the daylighting illuminance increasing, the lighting energy use dropped down gradually from the rated power of 56 W to 5.6 W when the lighting power multiplier reduced to 0.1. Compared with a normal glass window with the interior shading blind always on, the PV-DSF can save 53% and 26% lighting energy use on January 5 and December 9, respectively. Thus, making full use of the daylighting illuminance provided by semi-transparent PV modules is an effective way to considerably reduce the use of artificial lighting electricity.

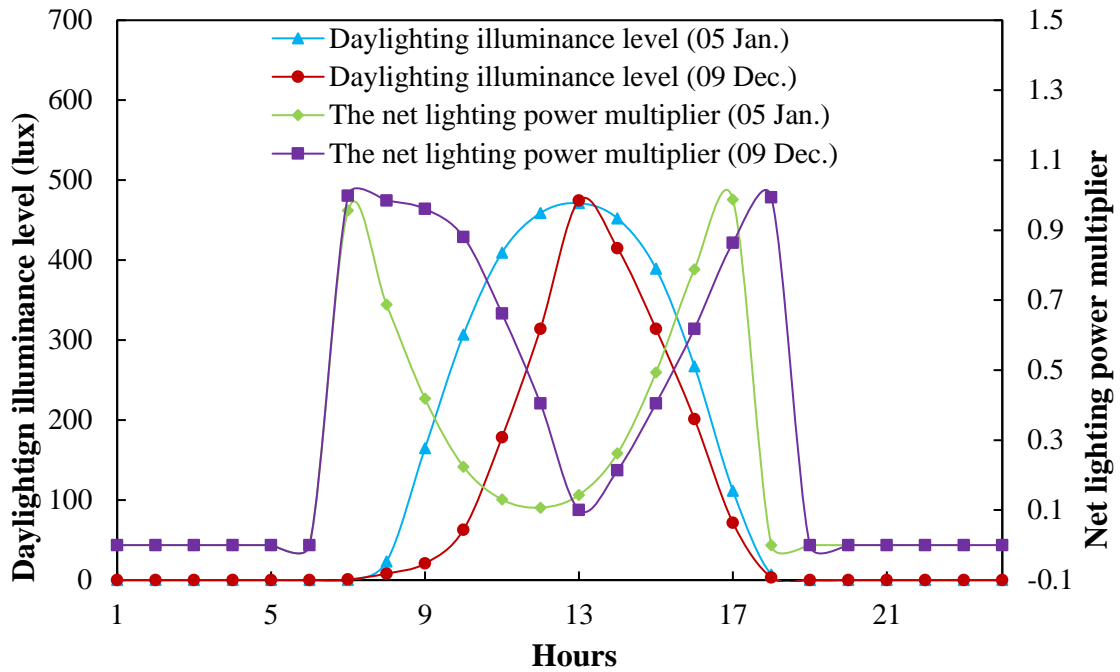


Figure 16. The daylighting illuminance level and the corresponding daylighting lighting power multiplier on December 9 and January 5

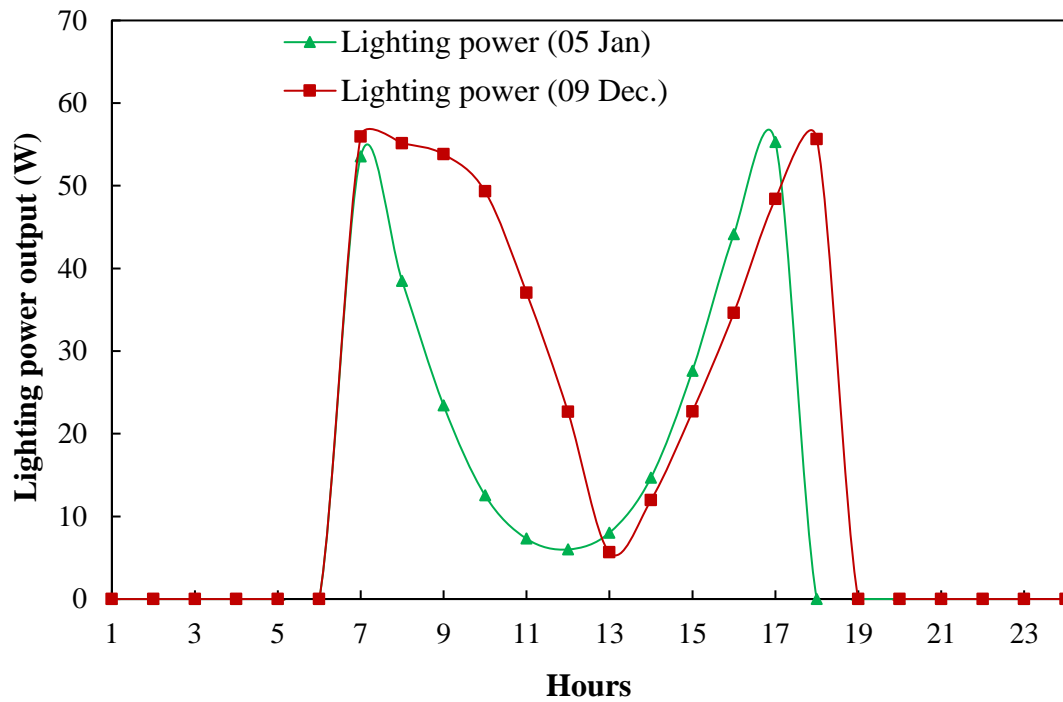


Figure 17. The hourly lighting power consumption on December 9 and January 5

5.4 Validation of Heat Gains through the PV-DSF

The simulated heat gain of the internal window of the PV- DSF was also validated against the measured heat flux, which was recorded by a heat flux meter. As shown in Figure 18, the simulated heat gain slightly overestimated the true heat gain at afternoons. It looks like there is an ahead of time for the measured data because, as we know, the peak heat gain through a south-facing window usually occurs at 1-2 PM (coincide with the peak simulation result) rather than at 12-1 PM. The main reason resulting in the ahead of time of the peak measured data and the overestimation of the simulated heat gain were probably due to the interior wall and the asymmetric installation location of the heat flux sensor. In order to conduct other comparative testing, an interior wall was set in the cavity that time. As the heat flux meter was attached on the right side window, sunlight in the morning was able to pass through the slat gaps of the upper louver and directly shine on the sensor, but in the afternoon the sunlight was obstructed by the interior wall, resulting in the decrease of heat flux at afternoon. Also due to the obstruction of the interior wall, the measured peak heat gain occurred ahead of time than that of the simulated result. If there is no interior wall, the daily peak of measured data would occur later, say at 2 PM. However, this interior wall was not considered in the simulation model, and the sunlight was not obstructed at afternoon in the model, thus the simulated heat gain was always higher than the measured data at afternoons on sunny days. In addition, as the indoor air temperature was higher than the ambient air temperature at night, the values of measured heat flux via the PV-DSF were negative, while the simulated results were zero because reverse heat flow can't be

calculated in this model. In general, although there is a certain degree of error between the simulated and measured heat fluxes, the heat transfer models in EnergyPlus are good enough to represent and simulate the PV-DSF heat transfer. The MAPE between the simulated and measured heat gains from March 6 to March 9 was 15%.

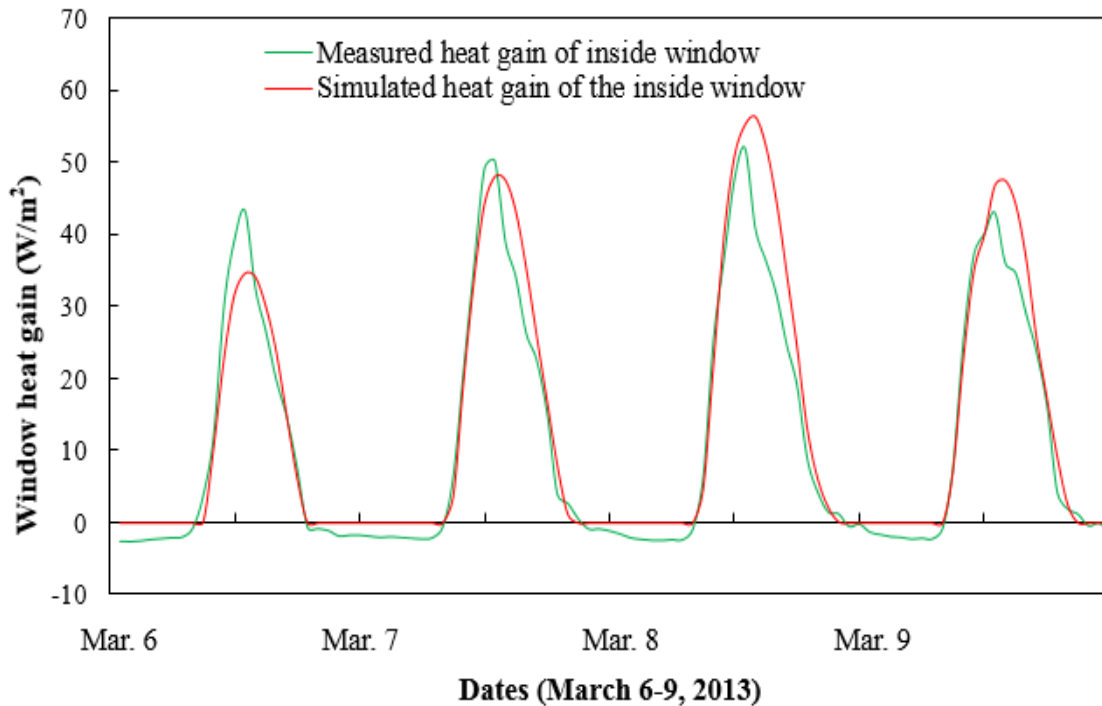


Figure 18. Comparison of the simulated heat gain and the measured heat gain

5.5 Validation of Daily Energy Output

Finally we consider the validation of the accuracy of the Sandia Array Performance Model (SAPM) using the measured daily energy output of the PV-DSF. In the PV-DSF test bed, the DC power generated by the PV modules was converted into AC power, with the same voltage and frequency as the utility grid electricity, by micro-inverters, whose characteristics were given in Table 4. The daily AC energy output was measured and

recorded by the micro-inverter. For the PV-DSF model in EnergyPlus, the PV module's energy output was simulated by the SAPM with a given performance ratio (PR) of the PV system. The performance ratio (PR) is stated as percentage and describes the relationship between the actual and theoretical energy outputs of a PV system. It shows the proportion of the energy that is actually available for exporting to the grid after deduction of energy loss (e.g. due to AC, DC losses and inverter loss). According to [42-43], the energy losses in this study was assumed to be constituted by 4.44% DC losses (including 2% mismatch loss, 0.5% connection loss and 2% DC wiring loss) and 7.732% AC losses (including 6.8% inverter loss and 1% AC wiring loss), the total energy loss from DC to AC power output was about 12%. Thus, the PR was determined to be 0.88, which is coinciding with a similar a-Si PV system in previous study [44].

The measured and simulated monthly AC power generations during the experimental campaign were compared in Table 5. To validate the SAPM model's accuracy on predicting annual power generation, the model estimates and measured data were compared using mean-bias-error (MBE), mean-absolute-error (MAE) and root-mean-square-error (RMSE) statistics, and the results are 0.14%, 2.13% and 2.47%, respectively.

Table 5 Comparison of measured and simulated monthly AC power generations

Months	Measured AC power generation (kWh)	Simulated AC power generation (kWh)
October	11.46	11.19
November	7.38	7.4
December	9.12	9.27
January	13.56	13.96
February	8.66	8.43

The SAPM model's accuracy was also compared with other models in previous studies. As shown in Table 6, except for the a-Si/x-Si HIT solar cell, the SAPM model made the lowest estimation errors, few of PV simulation models, so far reported, can achieve such high accuracy for a-Si PV modules. Although the Power Temperature Coefficient Model, PVFORM Model and Bilinear Interpolation Model presented very good prediction accuracy for the a-Si/x-Si HIT solar cell, these three models also made big errors for predicting the tripe junction a-Si solar cell.

Table 6 Comparisons of modelling errors between the SAPM model and other models

Models	Model estimation errors	Solar cell types	References
Back Temperature method	+3.4% (MBE)	a-Si (double-junction)	[45]
Site Specific Energy method	+1.8% (MBE)	a-Si (double-junction)	
MOTHERPV method	+3.4% (MBE)	a-Si (double-junction)	
On-line Simulator method	+6.8% (MBE)	a-Si (double-junction)	
TRW Equation	+6.0~+15.0% (RMSE)	a-Si (tripe-junction)	
5-Parameter model	+6% (RMSE)	a-Si (tripe-junction)	[46]
7-Parameter model	+5% (RMSE)	a-Si (tripe-junction)	[47]
Power Temperature Coefficient model	-2.6%/1.1% (MBE) +3.2%/1.4% (MAE) +4.5%/1.7% (RMSE)	a-Si (tripe-junction) a-Si/x-Si HIT	[48]
PVFORM model	-3.5%/0.1% (MBE)	a-Si (tripe-junction)	

	+3.9%/1.7% (MAE)	a-Si/x-Si HIT
	+4.9%/2.1% (RMSE)	
Bilinear	-2.0%/0.2% (MBE)	a-Si (tripe-junction)
Interpolation model	+3.3%/0.7% (MAE)	a-Si/x-Si HIT
	+4.4%/1.0% (RMSE)	
SAPM (this study)	+0.14% (MBE)	a-Si (double-junction)
	+2.13% (MAE)	
	+2.47% (RMSE)	

Two months with the highest monthly energy output, viz. October 2012 and January 2013, were chosen to compare the simulated and measured daily AC energy output. As shown in Figures 19 and 20, the SAPM accurately simulated the daily energy output of the PV-DSF with the 39 special pre-determined coefficients. The measured monthly AC energy output was 11.46 kWh in October 2012, while the simulated value was 11.19 kWh. The error is only 2.4%. Similarly, the measured monthly AC energy output was 13.56 kWh in January 2013, while the simulated value was 13.96 kWh, an error of 3%. Such a high level of accuracy for the monthly energy output prediction indicates that the SAPM fully qualifies for use in simulating the annual energy output performance of the a-Si PV-DSF.

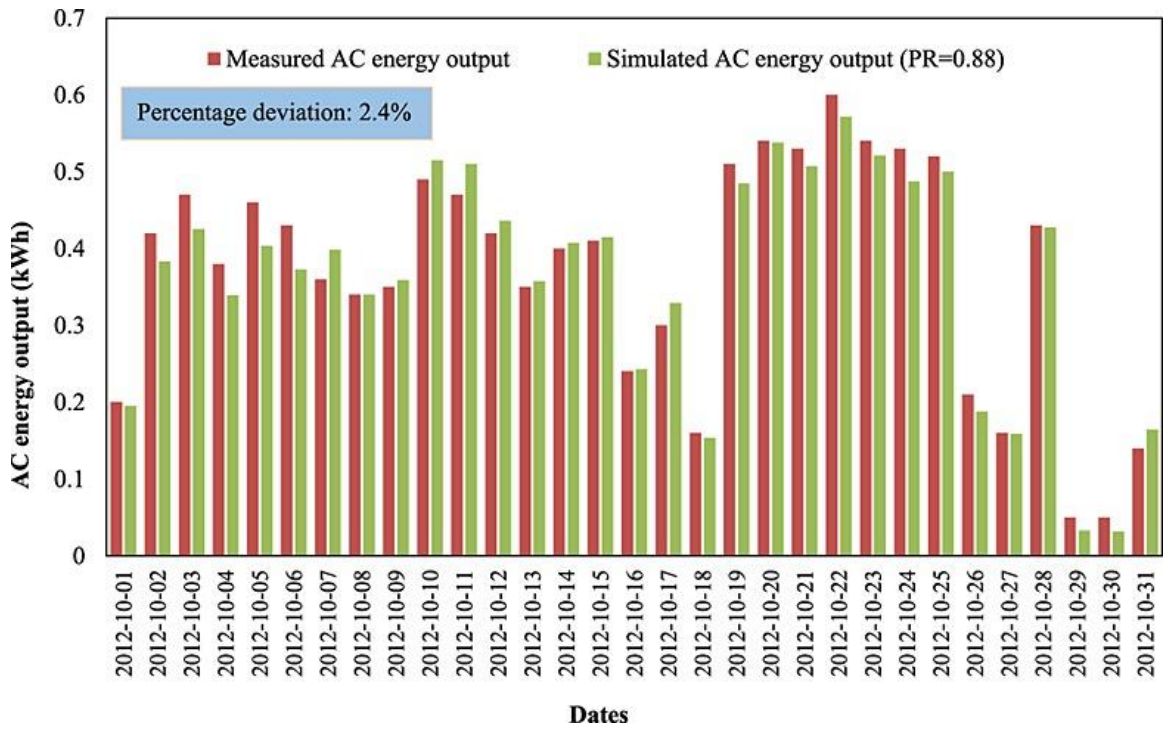


Figure 19. Comparison of the simulated daily energy output and the measured one in October 2012

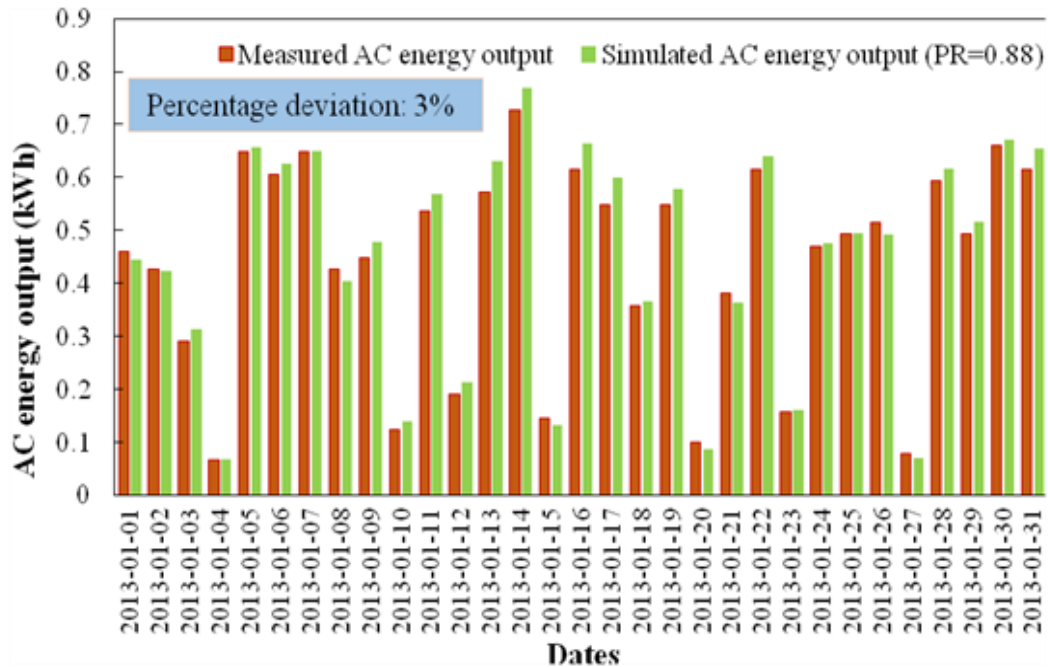


Figure 20. Comparison of the simulated daily energy output and the measured one in January 2013

6. Conclusions

A comprehensive simulation model based on the EnergyPlus software has been developed in this study to simulate the overall energy performance of a ventilated semi-transparent PV-DSF, taking into account the thermal, daylighting and dynamic power output performances of the full façade system simultaneously. The physical characteristics of the semi-transparent a-Si PV module were measured in the laboratory. The transmittance of the semi-transparent PV module was about 7% in the visible light range, and its thermal conductivity and infrared emittance were 0.48 ± 0.01 (W/(m·K)) (with temperature difference of 25 °C) and 0.853, respectively.

A PV-DSF model representative of the real PV-DSF was developed in EnergyPlus. Four openable windows with interior venetian blinds were adopted in the PV-DSF model

to represent the inlet and outlet louvers of the real PV-DSF. This approximate process for the louvers was indirectly proved to be a reasonable solution. The interactions among thermal, power and daylighting performances were reasonably well modelled by coupling the heat transfer model, airflow network model, Sandia Array Performance Model (SAPM) and daylighting model in EnergyPlus.

A long term outdoor experimental test was carried out to validate the various sub-model. The hourly simulation results of PV module temperature, heat gain, daylighting illuminance and power output were compared with the measured data. The MAPEs between the simulation results and the measured data were also calculated to evaluate the accuracy of the model. In general, the simulation results agreed well with the measured data with small difference for heat gain that was analyzed in the text. In particular, the root mean square error (RMSE) between the simulated monthly AC power output and the measured data was as low as 2.47%. Such a high accuracy indicated that the SAPM is well able to simulate the annual energy output performance of a PV-DSF. The validation results indicated that the simulation model developed can accurately simulate the overall energy performance of a semi-transparent PV-DSF considering both its energetic impacts on building energy use for heating, cooling and lighting as well as its power generation capability.

Although this model was developed based on a low transmittance PV module and was only validated in Hong Kong in this study, it should be independent on climate conditions and also suitable for other PV modules with different transmittances. Thus, this model can be used in the future for carrying out optimum design and sensitivity analysis for PV-DSFs in different climate zones and with different building characteristics. The methodology

developed in this study provides a favorable reference for modelling other kinds of semi-transparent thin-film PV (STPV) windows or facades.

Acknowledgements

The authors appreciate the financial supports provided by the Public Policy Research (PPR) Funding Scheme 2013/14 (PPR Project: 2013.A6.010.13A) of the Hong Kong Special Administrative Region (HKSAR), the Hong Kong Construction Industry Council Research Fund (CIC Project: K-ZJK1) and the Hong Kong Housing Authority Research Fund (Project no. K-ZJHE).

References:

- [1] Hong Kong Electrical and Mechanical Services Department (EMSD), Hong Kong energy end-use data 2012.
Available at http://www.emsd.gov.hk/emsd/e_download/pee/HKKEUD2012.pdf
- [2] Lu L, Law KM. Overall energy performance of semi-transparent single-glazed photovoltaic (PV) window for a typical office in Hong Kong. *Renewable Energy* 2013; 49: 250-254.
- [3] Miyazaki T, Akisawa A, Kashiwagi T. Energy savings of office buildings by the use of semi-transparent solar cells for windows. *Renewable Energy* 2005; 30: 281–304.
- [4] Chow TT, Li CY, Lin Z. Innovative solar windows for cooling-demand climate. *Solar Energy Materials and Solar Cells* 2010; 94:212-220.
- [5] Wong PW, Shimoda Y, Nonaka M, Inoue M, Mizuno M. Semi-transparent PV: Thermal performance, power generation, daylight modelling and energy saving potential in a residential application. *Renewable Energy* 2008; 33: 1024-1036.
- [6] Han J, Lu L, Yang HX. Thermal behavior of a novel type see-through glazing system with integrated PV cells. *Building and Environment* 2009; 44: 2129–2136.
- [7] Han J, Lu L, Yang HX. Numerical evaluation of the mixed convective heat transfer in a double-pane window integrated with see-through a-Si PV cells with low-e coatings. *Applied Energy* 2010; 87: 3431-3437.
- [8] Yoon JH, Shim SR, An YS, Lee KH. An experimental study on the annual surface temperature characteristics of amorphous silicon BIPV window. *Energy and Buildings* 2013; 62: 166–175.

- [9] Chen FZ, Wittkopf SK, Ng PK, Du H. Solar heat gain coefficient measurement of semi-transparent photovoltaic modules with indoor calorimetric hot box and solar simulator. *Energy and Buildings* 2012; 53: 74–84.
- [10] Bizzarri G, Gillott M, Belpoliti V. The potential of semitransparent photovoltaic devices for architectural Integration/The development of device performance and improvement of the indoor environmental quality and comfort through case-study application. *Sustainable Cities and Society* 2011; 1: 178-185.
- [11] Polo Lopez CS, Sangiorgi M. Comparison assessment of BIPV façade semi-transparent modules: further insights on human comfort conditions. International Conference on Solar Heating and Cooling for Buildings and Industry, 2013, Freiburg, Germany. *Energy Procedia* 2014; 48: 1419-1428.
- [12] Fung YY, Yang HX. Study on thermal performance of semi-transparent building-integrated photovoltaic glazings. *Energy and Buildings* 2008; 40: 341-350.
- [13] Park KE, Kang GH, Kim HI, Yu GJ, Kim JT. Analysis of thermal and electrical performance of semi-transparent photovoltaic (PV) module. *Energy* 2010; 35: 2681-2687.
- [14] Xu S, Liao W, Huang J, Kang J. Optimal PV cell coverage ratio for semi-transparent photovoltaic on office building facades in central China. *Energy and Buildings* 2014; 77: 130–138.
- [15] Yoon JH, Song JH, Lee SJ. Practical application of building integrated photovoltaic (BIPV) system using transparent amorphous silicon thin-film PV module. *Solar Energy* 2011; 85: 723-733.
- [16] Ng PK, Mithraratne N. Lifetime performance of semi-transparent building-integrated photovoltaic (BIPV) glazing systems in the tropics. *Renewable and Sustainable Energy Reviews* 2014; 31: 736-745.
- [17] Chow TT, Fong KF, He W, Lin Z, Chan ALS. Performance evaluation of a PV ventilated window applying to office building of Hong Kong. *Energy and Buildings* 2007; 39: 643-650.
- [18] Product manual of Hanergy, 2015.
<<http://www.hanergy.com/en/news/datadownload.html>>
- [19] Personal communications with Hanergy company.
- [20] Product Catalog of Advanced Solar Power (ASP), Version 1404.
<<http://www.adv solarpower.com/index.php/en/-jdownload/viewcategory/8->>

- [21] Li D, Lam T, Chan W, Mak A. Energy and cost analysis of semi-transparent photovoltaic in office buildings. *Applied Energy* 2009; 86: 722-729.
- [22] Olivieri L, Caamano-Martín E, Moralejo-Vazquez FJ, Martin-Chivelet N, Olivieri F, Neila-Gonzalez FJ. Energy saving potential of semi-transparent photovoltaic elements for building integration. *Energy* 2014; 76: 572-583.
- [23] Didone EL, Wagner A. Semi-transparent PV windows: A study for office buildings in Brazil. *Energy and Buildings* 2013; 67: 136–142.
- [24] Olivieri L, Caamano-Martina E, Olivieri F, Neila J. Integral energy performance characterization of semi-transparent photovoltaic elements for building integration under real operation conditions. *Energy and Buildings* 2014; 68: 280–291.
- [25] Peng JQ, Lu L, Yang HX. An experimental study of the thermal performance of a novel photovoltaic double-skin facade in Hong Kong. *Solar Energy* 2013; 97: 293-304.
- [26] Peng JQ, Lu L, Yang HX, Ma T. Comparative study of the thermal and power performances of a semi-transparent photovoltaic façade under different ventilation modes. *Applied Energy*, In Press, Available online 24 October 2014.
- [27] EnergyPlus Engineering Reference. The Reference to EnergyPlus Calculations. US Department of Energy, 2014.
- [28] Devices and Services, Emissometer with Scaling Digital Voltmeter Model AE1 RD1. Devices and Services Company, 2014.
- [29] Mitchell R., Kohler C., Klems J., Rubin M, Arasteh D. WINDOW 6.1 / THERM 6.1 Research Version User Manual. Lawrence Berkeley National Laboratory, US. 2006.
- [30] Hopkinson RG, Longmore J, Petherbridge P. An Empirical Formula for the Computation of the Indirect Component of Daylight Factors. *Transactions of the Illumination Engineering Society* 1954; 19(7): 201-218.
- [31] Lynes JA. Principles of Natural Lighting. Applied Science Publishers Ltd., London, p.129. 1968.
- [32] Paul J. Littlefair. The luminous efficacy of daylight: a review. *Lighting Research and Technology* 1985; 17: 162–182.
- [33] Energy Efficiency of LEDs. Building technologies program solid-state lighting technology fact sheet. Energy Efficiency and Renewable Energy. US Department of Energy, 2013.
<http://www.hi-led.eu/wp-content/themes/hiled/pdf/led_energy_efficiency.pdf>

- [34] King D, Boyson W, Kratochvill J. Photovoltaic Array Performance Model. Sandia Report 2004-3535, Sandia National Laboratories, Albuquerque, NM. 2004.
- [35] King D, Kratochvil J, Boyson W. Measuring Solar Spectral and Angle-of-Incidence Effects on PV Modules and Solar Irradiance Sensors. *26th IEEE PV Specialists Conference* 1997: 1113-1116.
- [36] King D, Kratochvil J, Boyson W. Temperature Coefficients for PV Modules and Arrays: Measurement Methods, Difficulties, and Results. *26th IEEE PV Specialists Conference* 1997: 1183-1186.
- [37] Hansen C, Stein J, Miller S, Boyson W, Kratochvil J, King D. Parameter Uncertainty in the Sandia Array Performance Model for Flat-Plate Crystalline Silicon Modules. *37th IEEE Photovoltaic Specialist Conference* 2011: 3138-3143.
- [38] Peng JQ, Lu L, Yang HX, Ma T. Validation of the Sandia model with indoor and outdoor measurements for semi-transparent amorphous silicon PV modules. *Renewable Energy* 2015; 80:316-323.
- [39] Hyndman RJ, Koehler AB. Another look at measures of forecast accuracy. *International Journal of Forecasting* 2006; 22 (4): 679–688.
- [40] Illuminating Engineering Society of North America (IESNA), *Lighting Handbook* (9th Edition.), Illuminating Engineering, 2000.
- [41] Hong Kong Electrical and Mechanical Services Department. *Task Lighting Design*. Energy Efficiency Office, 2012.
- [42] Marion B, Adelstein J, Boyle K, et al. Performance Parameters for Grid-Connected PV Systems. *The 31st IEEE Photovoltaics Specialists Conference and Exhibition*, Florida, United States, January 3-7, 2005.
- [43] Help manual of the System Advisor Model (SAM). National Renewable Energy Laboratory, 2014.
- [44] Chianese D, Bernasconi A, Friesen G, et al. Quality and energy yield of modules and photovoltaic plants. Final Report, August 2008.
<<http://www.isaac.supsi.ch>>
- [45] Williams SR. Site Specific Energy Prediction for Photovoltaic Devices. PhD Dissertation of Loughborough University, United Kingdom, 2009.
- [46] De Soto W. Improvement and Validation of a Model for Photovoltaic Array Performance. Master Dissertation of University of Wisconsin-Madison, United States, 2004.

- [47] Boyd MT. Evaluation and Validation of Equivalent Circuit Photovoltaic Solar Cell Performance Models. Master Dissertation of University of Wisconsin-Madison, United States, 2010.
- [48] Marion B. Comparison of Predictive Models for Photovoltaic Module Performance. *The 33rd IEEE Photovoltaic Specialists Conference*, San Diego, California, United States, May 11–16, 2008

TABLE CAPTIONS

Table 1 Key dimension parameters of the PV-DSF model

Table 2 Key physical properties of the glasses used

Table 3 Thermal properties of the wall

Table 4 The key experimental instruments and their specifications

Table 5 Comparison of measured and simulated monthly AC power generations

Table 6 Comparisons of modelling errors between the SAPM model and other models

Table 1 Key dimension parameters of the PV-DSF model

Parameters	Value
Width of the office room	2.32 m
Depth of the office room	2.3 m
Height of the office room	2.5 m
Width of PV module	1.1 m
Height of PV module	1.3 m
Thickness of PV module	0.008 m
Width of louver	1.1 m
Height of louver	0.45 m
Depth of air flow cavity	0.4 m
Window wall ratio	0.6

Table 2 Key physical properties of the glasses used

Glass ID	NFRC 411	NFRC 412
Glass type	Clear float glass	Clear float glass
Thickness (mm)	2.24	3.0
Transmittance of visible	0.9	0.9
Transmittance of solar light	0.856	0.838
Emissivity	0.84	0.84
Thermal conductivity	1	1

Table 3 Thermal properties of the wall

Items	Wall
Materials	Steel sheet (1.59 mm)+ Expanded Polystyrene (48.3 mm)+ Steel sheet (1.59 mm)
Thickness (mm)	51
U-factor (W/m ² /k)	0.62
R-value (m ² /k/W)	1.60

Table 4 The key experimental instruments and their specifications

Experimental Equipment	Manufacturer and model	Sensitivity and/or technical data	Measurement uncertainty
Weather station	Thies Clima	Wind speed: 0.1m/s; Wind direction: 1° ; Temperature: 0.1°C; Humidity:0.1%;	Nil
Pyranometers	EKO instruments (MS-802)	Sensitivity: about 7 $\mu\text{V}/(\text{W}/\text{m}^2)$;	Non-linearity<0.2 % (at 1000W/m ²);
Thermocouples	RS components (T type thermocouple)	Temperature range: -200 ~ 350°C;	- 40°C < t< 120°C = $\pm 1.5^\circ\text{C}$;
Conductive heat flux meters	Captec Enterprise (HS-30)	Sensitivity: 2.5 $\mu\text{V}/(\text{W}/\text{m}^2)$; Response time: 0.3 seconds;	<3%;
Data logger	Graphtec (GL820 Midi DataLogger)	Accepts Voltage (20mv to 50V), temperature, humidity, pulse and logic signals;	The minimum resolutions are 1 μV and 0.1 °C;
Light meter	TES (1336A)	Resolution: 0.01 Lux; Sensor: Silicon photo diode	$\pm (3\% \text{ rdg} + 5\text{dgts})$ (calibrated to standard incandescent lamp, 2856 K);
Micro-inverter	Involar (MAC250B)	Recommended Input Power (STC): 250W/200W~260W; DC voltage operating range: 60V~150V; MPPT Voltage Range: 72V~120V; Maximum DC Current: 3.47A	Power Factor>0.99; Peak Inverter Efficiency: 94.5%; CEC Weighted Efficiency: 93.2%.

Table 5 Comparison of measured and simulated monthly AC power generations

Months	Measured AC power generation (kWh)	Simulated AC power generation (kWh)
October	11.46	11.19
November	7.38	7.4
December	9.12	9.27
January	13.56	13.96
February	8.66	8.43

Table 6 Comparisons of modelling errors between the SAPM model and other models

Models	Model estimation errors	Solar cell types	References
Back Temperature method	+3.4% (MBE)	a-Si (double-junction)	[45]
Site Specific Energy method	+1.8% (MBE)	a-Si (double-junction)	
MOTHERPV method	+3.4% (MBE)	a-Si (double-junction)	
On-line Simulator method	+6.8% (MBE)	a-Si (double-junction)	
TRW Equation	+6.0~+15.0% (RMSE)	a-Si (tripe-junction)	
5-Parameter model	+6% (RMSE)	a-Si (tripe-junction)	[46]
7-Parameter model	+5% (RMSE)	a-Si (tripe-junction)	[47]
Power Temperature Coefficient model	-2.6%/1.1% (MBE) +3.2%/1.4% (MAE) +4.5%/1.7% (RMSE)	a-Si (tripe-junction) a-Si/x-Si HIT	[48]
PVFORM model	-3.5%/0.1% (MBE) +3.9%/1.7% (MAE) +4.9%/2.1% (RMSE)	a-Si (tripe-junction) a-Si/x-Si HIT	
Bilinear Interpolation model	-2.0%/0.2% (MBE) +3.3%/0.7% (MAE) +4.4%/1.0% (RMSE)	a-Si (tripe-junction) a-Si/x-Si HIT	
SAPM (this study)	+0.14% (MBE) +2.13% (MAE) +2.47% (RMSE)	a-Si (double-junction)	